Rolling Contact fatigue Defects and a New Approach to Rail Material Management

Róbert Horváth[1,*], Éva Majorosné Lublóy[2], Cecília Szigeti[3] and Zoltán Major[1]

[1]Széchenyi István University,
Department of Transport Infrastructure and Water Resources Engineering
Egyetem tér 1, H-9026 Győr, Hungary
{horvath.robert,majorz}@sze.hu

[2] Budapest University of Technology and Economics,
Department of Construction Materials and Technologies
Műegyetem rakpart 3, H-1111 Budapest, Hungary
lubloy.eva@emk.bme.hu

[3] Budapest Metropolitan University, Institute of Sustainable Studies
Nagy Lajos király útja 1-9, H-1148 Budapest, Hungary
cszigeti@metropolitan.hu
[*]Corresponding author e-mail: horvath.robert@sze.hu

Abstract: This article describes the current method of calculating the Hertzian contact stress and the corresponding shear stress occurring in the rail head at the rail-wheel contact and highlights the false sense of security that this approach creates among experts. The authors then present a method that is easy to implement in spreadsheet software and provides realistic results. In light of the results obtained, it is shown that it is not possible to prevent defects induced by the occurring stresses but only to keep them within limits by means of rail machining, which is a realistic objective, without significantly limiting the throughput capacity of the railway track. The combined effects of rail machining and natural wear cause the cross-sectional area and inertia and thus, the load-bearing capacity of the rails to decrease continuously. If the limit is exceeded, the rails may be installed again in less heavily used track sections and continue functioning. At the end of their service life, the track owner sells them as used rail scrap. If possible, recasting them as electro-steels, can significantly reduce the production costs and the amount of CO2 emitted during production.

Keywords: rail; contact stress; RCF defects; steel; recycling

1 Introduction

The relevance and environmentally friendly operation of rail transport in the 21st Century is unquestionable: for passenger transport, mainly for distances of 500-1000 km, and for freight transport, mainly over long distances. Several scientific articles were published to study railway vehicles [1] and various structural elements of ballasted and ballastless tracks, such as rails [2] [3] and rail joints [4], rail dampers [5] [6], sleepers [7] [8], crushed stone ballast [9] [10], granular supplementary layers [11] [12], substructure, etc. Rail technology and infrastructure innovations have made rail transport a key component in reducing greenhouse gas emissions. Continued research and development in this field are essential for advancing sustainable transportation solutions. The current paper deals with the rails and their special failures.

Over the last forty-five years, European railways have significantly progressed in traction vehicles, mainly in speed and axle load. Modern traction vehicles control increasing starting tractive efforts in the macroslip range. These improvements were necessary due to the need for higher axle loads with rising design speeds. Passenger trains on some European railways reached over 300 km/h, with static axle loads at 225 kN. These demands required optimal track conditions, as studied by Sadri and Steenbergen [13]. Transport throughput, measured by gross tonnage, significantly impacts wheel and rail wear. A 50% performance increase was projected for 2009-2025. This demand drove improvements in railway tracks, with new constructions utilizing 60 kg/km rails and enhanced material properties to reduce wear and maintenance costs. However, new defect phenomena, such as rolling contact fatigue (RCF) defects, have emerged, replacing rail breakage. These defects have been extensively studied [14] [15], leading to advancements in rail diagnostics and maintenance strategies.

Rail professionals often encounter various rail defects and are familiar with Hertzian contact stress in rail-wheel contact. The calculated value of this stress is an average and does not represent the maximum stress, posing potential safety risks. This article presents an exact method for calculating stresses, revealing that head checks, the most common rolling contact defect, are unavoidable. Conscious rail maintenance is crucial for safe operation. Rail maintenance methods, such as grinding and milling, cause natural wear and artificial material degradation, but recycled rails can still be used at reduced parameter values. Popović et al. discussed rail grinding in detail [16].

A robust rail network is crucial for logistical capabilities and serves as a vital alternative to road transport, essential for reducing greenhouse gas emissions [17, 18]. This need applies to both domestic and international networks [19] [20]. There is a positive correlation between railway infrastructure investments and socio-economic development [21]. Developing rail transport addresses the social and

economic challenges of the 21st Century while meeting environmental and economic requirements [22-24].

The current article examines the environmental and economic impacts of rails, the most expensive element of railway tracks, from production to recycling. According to a Spanish case study, infrastructure construction accounts for 75% of life-cycle carbon emissions [25]. In Hungary, high-alloy rail steel is sold as scrap at the end of its life, losing its excellent properties when mixed with normal steels. The article proposes an environmentally sound use of waste rail material, forming a basis for further research. Circular management in other sectors, like agriculture, offers a model for applying this approach to infrastructure construction and maintenance [26-28].

2 Theory

According to the commonly used Hertzian formula, the value of the contact stress depends only on the wheel load and the radius of the wheel. This relationship is illustrated in Eq. (1) [29]:

$$q_{mean} = 1374 \cdot \sqrt{\frac{Q}{r}} \tag{1}$$

in which q_{mean} is the average value of the contact stress [N/mm^2], Q is the wheel load [kN], and r is the wheel tread radius [mm]. Using the correlation In Eq. (1), the maximum value of the shear stress in the rail head can be calculated using Eq. (2) [29], considering the Poisson's ratio of the rail material (v = 0.3). It should be noted that, once again, a correlation based on an approximation at the expense of safety is presented, which incorrectly derives the maximum shear stress from the average value of the contact stress. The maximum value is written in Eq. (2).

$$\tau_{max} = 0.3 \cdot q_{mean} = 412 \cdot \sqrt{\frac{Q}{r}} \tag{2}$$

in which τ_{max}: maximum shear stress in the rail head [N/mm^2].

Eq. (1), presented for contact stress, is a further simplification of the reduced formula of the original Hertzian correlation. The original simplified formula was created by Eisenmann [29] in the form corresponding to Eq. (3). This expression also provides an average value similar to Eq. (1).

$$q_{mean} = \sqrt{\frac{\pi \cdot E}{64 \cdot (1-v^2)} \cdot \frac{Q}{r \cdot b}} \tag{3}$$

in which b is the half-width of the contact ellipse [mm], E is the modulus of elasticity of the rail material [N/mm^2], v is the Poisson's ratio of the rail material.

By substituting the following values into Eq. (3), Eq. (1) is received [29], a re-simplification based on practical experience: E=210 kN/mm^2, ν=0.3, b=6 mm.

If someone asks the question why new defect phenomena have developed compared to the previous ones, someone can rightly think of increased loads, but this would be too simple an answer since the railways have taken countermeasures, increased the cross-section, tensile strength, and hardness of the rails, and created new rail and wheel profiles. However, looking at the theory used in the calculations, the flaw in this approximation becomes apparent since, while real values are available for the material properties, a highly hypothetical approximation has been used for the half-width of the contact ellipse. Forgetting this approximation, the profession has now noted and applied only Eq. (1), which gives sufficiently reassuring results. However, life has not proved this to be true since a large part of the rail network is subject to rolling contact defects. An example of this is shown in Fig. 1.

Figure 1
Rails affected by head checks (HC) and squat defects

In [30], Kazinczy examines the problem based on a cylinder-cylinder contact model that is closer to the real conditions, the principle of which is illustrated in Figure 2.

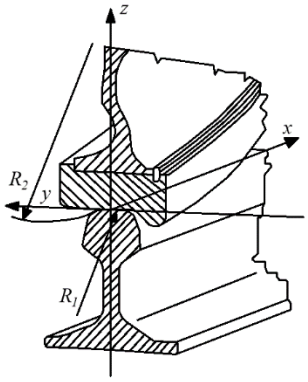

Figure 2
Rail-wheel contact in a Hertzian cylinder-cylinder model (on the basis of [30])

The article points out that the stresses calculated this way can be significantly higher than those determined by approximate formulae. The disadvantage of the method is that it only gives accurate results for conical wheels modeled on the original railway wheel and for other wheel profiles where the contact with the rail is on the conical surface. This solution can only give an approximate result for wheel profiles with a complex basket curve design.

In the following, the authors will present a method to calculate the exact geometry and stresses of the contact of today's complex wheel profiles and rail profiles. The calculation of the stresses at the contact between rails and wheel profiles of different wear must also be addressed and will be the subject of future research.

3 Calculation Method

In order to present the original Hertzian calculation method and its practical application, the authors consulted [31]. In the current article, the derivation of the limiting values on the resistance side is described in addition to the quantity on the stress side, which is derived partly from the work of Esveld [29] and partly from the book [32]. In [31], the authors show how to solve Hertz's original theory and offer methods that practicing engineers can apply. In this article, the authors do not intend to go into the theoretical background in detail but rather to illustrate its applicability. The authors follow the notation system of the referenced literature and introduce the authors' notation where appropriate.

The geometry of the contact surfaces is characterized by four radii values in the calculations, two of which are characteristic of the wheel and two of the rail head: 1) the wheel tread radius (R_{11}); 2) the radius of the rounding on the wheel rim at the contact point (R_{12}); 3) the radius of the rounding of the rail head at the contact point (R_{21}); 4) the vertical rounding radius of the rail (R_{22}).

Remarks: (i) the radius values are interpreted in millimeter dimensions; (ii) the rounding on the wheel tread is concave, so the radius value has a negative sign; (iii) if the contact occurs on the conical part of the wheel tread, a very large number must be used for the value of the radius (e.g., 10^{10} mm); (iv) the value of the vertical rounding radius of the rail is several orders of magnitude higher than the other quantities, its examination in practical calculations is negligible. In the case of a convex rounding arc, the value of the radius has a positive sign, while in the case of a concave rounding arc, it is negative.

In the first step of the calculation, the geometric quantities characteristic of the contact must be determined. In accordance with Eqs. (4-7), someone can calculate the main curvatures characteristic of the contacting bodies at the contact point, while their sum is calculated according to Eq. (8).

The main curvatures of the wheel at the contact point:

$$k_{11} = \frac{1}{R_{11}} \tag{4}$$

$$k_{12} = \frac{1}{R_{12}} \tag{5}$$

The main curvatures of the rail at the contact point:

$$k_{21} = \frac{1}{R_{21}} \tag{6}$$

$$k_{22} = \frac{1}{R_{22}} \tag{7}$$

The sum of the main curvatures at the contact point:

$$\Sigma k = k_{11} + k_{12} + k_{21} + k_{22} \tag{8}$$

Based on the defined curvatures, the auxiliary quantity Ω can be determined, which plays an essential role in the practical solution of the problem. Its calculation is summarized in Eq. (9).

$$\Omega = \frac{\sqrt{(k_{11}-k_{12})^2+(k_{21}-k_{22})^2+2\cdot(k_{11}-k_{12})\cdot(k_{21}-k_{22})\cdot cos(2\omega)}}{k_{11}+k_{12}+k_{21}+k_{22}} \tag{9}$$

In Eq. (9), there is only one unknown quantity, ω. This quantity represents the angle between the planes of the curvatures k_{11} and k_{21}. As the plane of curvature of the wheel tread and the plane of curvature of the rounding arc of the rail can be considered perpendicular to each other, the cosine of twice the angle value can be considered based on Eq. (10).

$$cos(2\omega) = -1 \tag{10}$$

Based on the geometric quantities, the contact must also be characterized from the material property side in the second step of the calculation. For this, someone needs to know the two contacting bodies' elastic modulus (E_1 and E_2) and Poisson's ratio (μ_1 and μ_2). Based on this, the elasticity constant of the contacting bodies can be calculated according to Eq. (11).

$$\eta = \frac{1-\mu_1^2}{E_1} + \frac{1-\mu_2^2}{E_2} \tag{11}$$

Remarks: (i) the elastic modulus values are interpreted in N/mm^2 dimensions; (ii) in the case of contacting bodies of the same material, the formula can be simplified according to Eq. (12).

$$\eta = 2 \cdot \frac{1-\mu^2}{E} \tag{12}$$

In the third step of the calculation, the maximum Hertzian stress can be determined, the convergence of the contacting bodies due to their elastic deformation, the maximum shear stress occurring in the rail head, and its location (depth) under the contact surface.

The maximum contact voltage (p_0) occurring at the contact point can be calculated based on Eq. (13) in a general way.

$$p_0 = \frac{3}{2} \cdot \frac{F}{\pi \cdot a \cdot b} \tag{13}$$

in which F is the wheel load [N]; a is the length of the semi-major axis of the contour ellipse [mm]; b is the length of the semi-minor axis of the contour ellipse [mm].

The length of the half-axes of a contour ellipse can be determined using Eqs. (14-15). The auxiliary quantities n_a and n_b in the formula can be taken from *Table 1* as a function of the auxiliary quantity Ω introduced earlier. A linear interpolation between the values in the table is applied according to the value of Ω.

$$a = n_a \cdot \sqrt[3]{\frac{3}{2} \cdot \frac{\eta \cdot F}{\Sigma k}} \tag{14}$$

$$b = n_b \cdot \sqrt[3]{\frac{3}{2} \cdot \frac{\eta \cdot F}{\Sigma k}} \tag{15}$$

Using the values in *Table 1*, the maximum Hertzian stress can be computed directly according to Eq. (16), as well as the convergence of the contacting bodies due to their elastic deformation according to Eq. (17). The notations used in the formulae are the same as before:

$$p_0 = n_p \cdot \frac{1}{\pi} \cdot \sqrt[3]{\frac{3}{2} \cdot \left(\frac{\Sigma k}{\eta}\right)^2 \cdot F} \tag{16}$$

$$\delta = n_\delta \cdot \frac{1}{\pi} \cdot \sqrt[3]{\frac{9}{4} \cdot \eta^2 \cdot \Sigma k \cdot F^2} \tag{17}$$

Based on the contact stress, Ponomarev et al. [31] concluded that for steel contacts, if the contact is elliptical, the value of the maximum shear stress in the rail head is practically independent of the ratio of the semi-axes and can be calculated according to Eq. (18).

$$\tau_{max} = 0.325 \cdot p_0 \tag{18}$$

Ponomarev et al. [31] also investigated the shear stress value on the surface. In their analysis, however, they found that its value is a quantity sensitive to the ratio of the semi-axes of the contour ellipse, and its maximum value is not greater than the value given by Eq. (19), which is much smaller than the value developed inside the rail head, but not negligible.

$$\tau_{max} = 0.200 \cdot p_0 \tag{19}$$

Remark: When considering the stresses on the surface, additional considerations are needed to take into account the effect of friction between the rail and the wheel.

This can cause the shear stress on the running surface to increase significantly and exacerbate the problem [31].

Table 1
Auxiliary quantities of the calculation method

Ω	η_a	η_b	η_p	η_δ	Ω	η_a	η_b	η_p	η_δ
0.0192	1.013	0.9873	0.9999	0.9999	0.7238	1.979	0.5938	0.8507	0.8451
0.0395	1.027	0.9742	0.9997	0.9997	0.7449	2.053	0.5808	0.8386	0.8320
0.0609	1.042	0.9606	0.9992	0.9992	0.7673	2.141	0.5665	0.8246	0.8168
0.0835	1.058	0.9465	0.9985	0.9985	0.7911	2.248	0.5505	0.8082	0.7990
0.1075	1.076	0.9318	0.9974	0.9974	0.8166	2.381	0.5325	0.7887	0.7775
0.1330	1.095	0.9165	0.9960	0.9960	0.8300	2.463	0.5224	0.7774	0.7650
0.1602	1.117	0.9005	0.9942	0.9942	0.8441	2.557	0.5114	0.7647	0.7509
0.1894	1.141	0.8873	0.9919	0.9919	0.8587	2.669	0.4993	0.7504	0.7349
0.2207	1.168	0.8660	0.9890	0.9889	0.8741	2.805	0.4858	0.7338	0.7163
0.2545	1.198	0.8472	0.9853	0.9852	0.8904	2.975	0.4704	0.7144	0.6943
0.2913	1.233	0.8271	0.9805	0.9804	0.9077	3.199	0.4524	0.6909	0.6675
0.3314	1.274	0.8056	0.9746	0.9744	0.9113	3.253	0.4484	0.6856	0.6613
0.3755	1.322	0.7822	0.9669	0.9667	0.9150	3.311	0.4442	0.6799	0.6549
0.4245	1.381	0.7565	0.9571	0.9566	0.9187	3.373	0.4398	0.6740	0.6481
0.4795	1.456	0.7278	0.9440	0.9432	0.9225	3.441	0.4352	0.6678	0.6409
0.4914	1.473	0.7216	0.9409	0.9400	0.9264	3.514	0.4304	0.6612	0.6333
0.5036	1.491	0.7152	0.9376	0.9366	0.9303	3.594	0.4253	0.6542	0.6251
0.5161	1.511	0.7086	0.9340	0.9329	0.9342	3.683	0.4199	0.6467	0.6164
0.5291	1.532	0.7019	0.9302	0.9290	0.9383	3.781	0.4142	0.6387	0.6071
0.5423	1.554	0.6949	0.9262	0.9248	0.9425	3.890	0.4080	0.6300	0.5970
0.5560	1.578	0.6876	0.9219	0.9203	0.9467	4.014	0.4014	0.6206	0.5860
0.5702	1.603	0.6801	0.9172	0.9155	0.9511	4.156	0.3942	0.6104	0.5741
0.5848	1.631	0.6723	0.9121	0.9102	0.9556	4.320	0.3864	0.5990	0.5608
0.5999	1.660	0.6642	0.9067	0.9045	0.9601	4.515	0.3777	0.5864	0.4560
0.6155	1.693	0.6557	0.9008	0.8983	0.9649	4.750	0.3680	0.5721	0.5292
0.6317	1.729	0.6468	0.8944	0.8916	0.9698	5.046	0.3568	0.5555	0.5096
0.6485	1.768	0.6374	0.8873	0.8841	0.9749	5.432	0.3436	0.5358	0.4864
0.6662	1.812	0.6276	0.8766	0.8759	0.9803	5.976	0.3273	0.5112	0.4574
0.6845	1.861	0.6171	0.8710	0.8668	0.9861	6.837	0.3058	0.4783	0.4186
0.7037	1.916	0.6059	0.8614	0.8566	0.9923	8.609	0.2722	0.4267	0.3579

4 Materials

The calculation presented here is a way to quantify the quantities that appear on the stress side. To do the same for the strength side, further literature research has been carried out, summarized in Section 5.

For practical tasks, very few limit values are available for the Hertzian stress. Chapter E of [32] deals with crane structures. Massányi [32] gives the value according to Eq. (20) for the calculation of the head width of a crane rail.

$$\sigma_{Hm} = 1.8 \cdot \sigma_B \tag{20}$$

in which σ_{Hm} is the permissible Hertzian stress [N/mm^2]; σ_B is the tensile strength of the rail [N/mm^2]. The authors do not attribute a safety factor to this value but calculate with a safety factor of n=3.3 for the required width of the rail head.

When calculating the shear stress limit, the design engineers are in a more fortunate situation since Esveld [29] also gives a limit value, which is illustrated in Eq. (21).

$$\tau_m = 0.5 \cdot \frac{\sigma_B}{\sqrt{3}} \tag{21}$$

in which τ_m is the permissible shear stress [N/mm^2]; σ_B is the tensile strength of the rail [N/mm^2]. This approach corresponds to a safety factor of n=2.0 in real life.

When calculating the shear stress limit, the design engineers are in a more fortunate situation.

Since the authors cannot clearly assign a safety factor to the Hertzian contact stress, they propose determining its limit value based on the maximum shear stress correlation. This solution is not based on an accepted engineering consensus but on the authors' ideas. When determining the limit value, the correlation between the maximum shear stress in the rail head and the Hertzian stress is first considered according to Eq. (18). In the limit situation, this quantity shall be equal to the shear stress limit value according to Eq. (21). By combining the two equations, the correlation is obtained given by Eq. (22), which, when calculated for the upper limit of the Hertzian stress, gives the correlation given by Eq. (23), which, simplified, gives the maximum permissible value of the contact voltage (p_0), as given by Eq. (24).

$$0.325 \cdot p_0 = 0.5 \cdot \frac{\sigma_B}{\sqrt{3}} \tag{22}$$

$$p_0 = \frac{0.5}{0.325} \cdot \frac{1}{\sqrt{3}} \cdot \sigma_B \tag{23}$$

$$p_0 = 0.8882 \cdot \sigma_B \tag{24}$$

In order to facilitate practical calculations, it is proposed to use the correlation in Eq. (27) for the Hertzian contact stress limit by simplifying the correlation in Eq. (26). The use of this value is also advantageous from a practical point of view because it implies that the value of the shear stress in the rail head is undoubtedly below the limit value and does not require a special test to verify compliance:

$$\sigma_{Hm} = 0.88 \cdot \sigma_B \tag{25}$$

For practical calculations, the limit values for each rail steel grade have been determined based on Eqs. (21) and (25), which are summarized in *Table 2*.

Table 2
Limit values specific to each rail material

Material	$R_{m,min}$ [N/mm^2]	A_5 [%]	σ_{Hm} [N/mm^2]	τ_m [N/mm^2]
UIC700*	680	14	598	196
UIC260(900A)*	880	10	774	254
UIC260 Mn(900B)*	880	10	774	254
UIC1100*	1080	9	950	312
R200**	680	14	598	196
R220**	770	12	677	222
R260**	880	10	774	254
R260 Mn**	880	10	774	254
R320 Cr**	1080	9	950	312
R350 HT**	1175	9	1034	339
R350 LHT**	1175	9	1034	339
R370 CrHT**	1280	9	1126	369
R400 HT**	1280	9	1126	369
*: according to the UIC leaflet 860-0 **: according to the EN 13674-1				

where:

$R_{m,min}$: minimum tensile strength of the rail steel [N/mm^2]

A_5: elongation at rupture of the rail steel [%]

σ_{Hm}: permissibleHertzian contact stress [N/mm^2]

τ_m: permissible shear stress [N/mm^2]

Esveld [29] also offers the possibility to determine the tensile strength based on the composition of the rail material to obtain the initial value, the method of which is shown in Eq. (26). To facilitate practical work, the authors also provide the correlations for the yield strength (see Eq. (27)) and the elongation at rupture Eq. (28) according to [29].

$$\sigma_u = 227 + 803 \cdot \%C + 87 \cdot \%Si + 115 \cdot \%Mn + 133 \cdot \%Cr + 891 \cdot \%P + 614 \cdot \%V \pm 19\ N/mm^2 \quad (26)$$

$$\sigma_y = 101 + 469 \cdot \%C + 36 \cdot \%Si + 85 \cdot \%Mn + 116 \cdot \%Cr + 0 \cdot \%P + 634 \cdot \%V \pm 21\ N/mm^2 \quad (27)$$

$$\delta_5 = 30.8 - 22.6 \cdot \%C - 1.7 \cdot \%Si + 0 \cdot \%Mn - 2.3 \cdot \%Cr + 0 \cdot \%P + 4.4 \cdot \%V \pm 0.9\ \% \quad (28)$$

where:

σ_u: tensile strength of the rail steel [N/mm^2]

σ_y: yield strength of the rail steel [N/mm^2]

δ_5: elongation at rupture of the rail steel [%]

%C: Carbon content of the rail steel [%]

%Si: Silicon content of the rail steel [%]

%Mn: Manganese content of the rail steel [%]

%Cr: Chrome content of the rail steel [%]

%P: Phosphorus content of the rail steel [%]

%V: Vanadium content of the rail steel [%]

The issue of elongation at rupture is considered relevant because one of the solutions to reduce the occurrence of RCF defects is to increase the tensile strength of the rail material. As can be seen, this solution can be effective since it can successfully increase the fatigue limit strength (see *Table 2*). However, it results in a more brittle steel material in the rail head, unfavorable for crack propagation. Béres and Unyi drew attention to this connection as early as 1978 [33]. Based on compact tension (CT) studies, they pointed out that the size of the defect that initiates fatigue failure decreases with increasing the hardness and strength of the rail material. It should be noted that the initial hardness of the rail head can be further increased by the cold rolling effect of the traffic load, which can lead to even more intense damage. An example of this was presented by Csizmazia and Horvát [34]. The sudden decrease in hardness value is typical for the immediate vicinity of the crack.

5 Results and Discussion

In order to validate the calculation method, the authors present and point out the relevance of the subject under study; they have used the data reported by Esveld [29], which is valid for a wheel load Q=60 kN for the geometric quantities under study. The calculated values are separated from the values reported by Esveld with the "/" sign in *Table 3*. The approximate values based on Eq. (1) are also given here.

Table 3
Calculated results

Case	**1**	**2**	**3**
Radius of the wheel [mm]	460	460	460
Curvature radius of the wheel profile [mm]	∞	–330	–330
Curvature radius of the rail profile [mm]	300	300	80
***a* [mm]** own / Esveld	6.0 / 6.1	14.2 / 14.6	7.0 / 7.1
***b* [mm]** own / Esveld	4.6 / 4.7	3.9 / 3.9	2.6 / 2.7
p_0 **[N/mm²]** own / Esveld	1044 / 1012	515 / 502	1557 / 1520
p_0 **[N/mm²]** based on Eq. (1)	496	496	496

Based on the tests performed and their results, it can be concluded that the presented method is sufficiently accurate and that the calculated contact stress values approximate the literature values from above. If someone examines the values that can be calculated using the approximate correlation, it can be found that it would be uniformly 496 N/mm^2. These approximate values illustrate how much pseudo-safety the approximate formula can provide compared to the real values. A comparison of the results obtained (see Table 3) with the limits summarized in Table 2 leads to a surprising result. It can be observed that the Hertzian stress value for the tapered design corresponding to the original rail wheel (case 1) requires sufficiently high-quality rail steel compared to the design corresponding to the wear profile (case 2). When the contact of the wear profile is applied to the track gauge corner (case 3), it is apparent that damage is sure to occur.

It was evident for the rail steel materials that the elongation at rupture decreases with increasing tensile strength, for which a value of less than 9% is not permissible. Thus, by intervening from the material side, the process cannot be eliminated, but only the rate of deterioration can be reduced.

Please note that wheel loads greater than 60 kN need to be examined in real conditions. From Eq. (12), it is evident that the resulting stress is proportional to the cube root of the wheel force. For an axle load of 225 kN and a theoretical wheel load of 112.5 kN (not including dynamic effects), multiplying the p_0 values in Table 3 by 1.23 gives the values that can be assumed under operating conditions, as shown in Eq. (29).

$$p_{0,(112.5kN)} = p_{0,(60kN)} \cdot \sqrt[3]{\frac{112.5}{60}} = p_{0,(60kN)} \cdot 1.23 \tag{29}$$

The result is usually 1284, 633, and 1915 N/mm^2, respectively. At these values, damage is almost inevitable, even in the 1st case. These RCF defects, which do not appear near the gauge corner but at the center line of the rail head, are Belgrospi and squat. While in case 3, the almost certain form of damage close to the track gauge corner is the Head Check (HC). In the authors' view, the calculation method presented is not in itself sufficient for a complex analysis. The wheel-rail contact stress problem should not be treated separately from the equivalent conicity analysis, as it can be used to explore the possible contact points and contact geometries. A precise knowledge of the rail and the wheel's material properties is indispensable to understanding the problem. A detailed study of the interrelationships will also determine the authors' direction in further research. Furthermore, it should be noted that the development of RCF-type defects under investigation can be positively influenced by the phenomenon of natural wear under certain conditions through the speed and extent of wear. By replacing this natural wear with engineering maintenance activities, a plannable rail machining can effectively deal with RCF defects, accepting the seemingly insoluble contradiction that, although the feeling of false safety can be eliminated by accurate calculation and the development of the defect can be predicted, without conscious improvement

activities, the profession must live with this and can only deal with the defect symptomatically. Depending on their resources, individual railway companies have been able to adapt to this possibility, sometimes more effectively and sometimes less effectively. The results achieved range widely from a preventive approach to "merely putting out local fires" and significantly impact the performance of the tracks. Given the above, it is not surprising that railway companies are working on different management strategies. An essential requirement is to ensure that maintenance is carried out adequately. An important task for track managers is to maintain the track profile's original shape and deal with RCF defects. Over the past decades, several research projects have addressed this issue, and regulations have been developed based on operator experience.

Regarding head check (HC) defects, it is also vital to present some high-resolution images taken during laboratory testing of a rail with hairline cracks. E.g., the paper [35] deals with the microscopic enlargement of the surface of an HC-damaged rail. In addition to microcracks, the surface also shows some spalling.

Transverse cracks penetrate deeply into the rail material. Without corrective grinding, further spalling is certain to occur, and deep crack penetration can ultimately cause rail breakage. It should be noted, however, that for the defects [35], the depth of damage calculated from the measurement by survey train is less than 2.5 mm, and this value is not the same as the actual depth that can be interpreted concerning the rail tread. Contact stress and maximum shear stress have an obvious role in the development of HC defects and in the change in the slope of the angle of penetration for the surface at a depth of about 3-5 mm, which is why it is essential to use a method as accurate as possible to calculate the rail stress to address the problem. If someone can identify the most relevant contact positions for RCF defects, a big step forward can be made in effectively dealing with this phenomenon.

Based on the calculated data, it is easy to see that the RCF defects under investigation will continue to cause problems. Their development cannot be prevented, but the defects that are developed can be temporarily reduced/eliminated.

The rail is the most expensive part of the railway track. Its manufacture and installation are major logistical and technical challenges since they involve moving and installing 120 m rails in one piece. The maintenance of sections affected by RCF defects requires a method that can remove the damaged parts to just the necessary extent. The basis of any modern maintenance strategy is a high level of measurement technology to detect defect locations and damage depths as accurately as possible [36]. In the Hungarian annual measurement programs, each railway line is subjected to one or two measurements: mechanical ultrasound, rail profile, equivalent conicity and eddy current ones, depending on the load. This combination is necessary because only by applying the different methods simultaneously can a proper picture of the depth and, thus, the severity of the defects be obtained. Once the measurement results have been processed, the rail treatment plan for the next

six months or one year is determined. Failure caused by RCF defects is inevitable on busy tracks without regular track maintenance (rail grinding with oscillating stones, rail grinding with rotating stones, and possibly rail milling). As the progression of HC defects penetrates steeply into the rail material after a certain defect depth (3-5 mm), only a defect removal procedure or rail replacement can repair the damaged rail. If the depth of the defects is not allowed to fall below the critical point, the service life of the rails can be increased by repeated minor interventions. If diagnostic and repair technologies are applied correctly in developing maintenance strategies for transport infrastructure, a significantly improved facility operation in terms of sustainability can be achieved. By extending the lifetime of individual infrastructure elements, in the authors' case, the rails, as long as possible, but not overusing them and minimizing life cycle costs, someone can also significantly reduce the environmental impact. Rails in their first use cycle will, at some point, reach a wear limit due to natural and artificial wear (grinding), above which no greater value can be permitted. These rails can still carry loads but at lower speeds and/or axle loads. When the reclaimed material is installed in such tracks, the rail maintenance process is restarted and continued for as long as the rails can be kept in service.

In the Hungarian practice, the rails are sold as general steel scrap at the end of their service life. In the authors' view, this sale is made by the owner of the railway network at a much lower value than the fair value, taking into account the highly alloyed nature of the rail material. This practice takes the rail material out of the real recycling loop and puts it back on the market as general steel, while the production of rail steel indicates the use of additional primary raw material. It is now widely accepted practice in Europe that some manufacturers are obliged to take their products back for processing at the end of their life. In order to ensure the recycling of railway rails, the secondary use of rail material can be ensured by adding contractual conditions to the contract between the operator and the suppliers of new rails. As the costs of loading, transport and storage of the replaced rail material have been incurred in the past just the same, the innovative solution does not necessarily entail additional costs and logistical tasks. If the recycling were to take place at a rail manufacturer, the manufacturer would then get back the used rail material, which they could reuse and make production more energy and environmentally friendly, reducing the need for primary raw material (the impact of material loss due to wear and rail grinding must always be taken into account), and thus be able to offer their product at a lower price.

The authors envisage that in the production of rail steel, it is expedient to produce electro-steel from secondary rail scrap in electric arc furnaces, effectively melting the high-alloy charged material (with the addition of alloying elements if necessary), followed by continuous casting to produce billets suitable for rolling [37]. The advantage of using arc furnaces is that they can be used effectively with up to 100% iron scrap charge. Another significant advantage over conventional production is that only the amount of energy needed for melting is required, and

thus, the process is less energy-intensive and emits less CO_2. Energy consumption can be reduced by almost one-third and CO_2 emissions by almost one-fifth [38].

The model can be built in an ascending system, whereby a significant part of the primary raw material consumption can be replaced by secondary raw material. The rails, which are otherwise sold as scrap iron, are processed together with other scrap materials. The costs of shredding, transporting and remelting will not impose any additional burden on producers, as they have already done so. If high alloy rail steel is, as we propose, to be fed exclusively into the production of rails, a significant proportion of the alloying elements will be retained, thereby reducing the cost of production and the environmental impact of manufacturing. In the initial phase, it is already possible for the production company to buy scrap rail material, even originating from other manufacturers from track owners. They are fortunate to obtain information about the rail material used for newly rolled rails from the rolling marks on the rail web, which also provide information about the manufacturer and the rolling time. Unfortunately, there are still old rails without rolling marks on the track. In this case, the results of a gas chromatography analysis of samples of the deposited reclaimed material provide reliable information on the composition of the material and its possible uses. The performance of recycled rails does not differ from that of conventionally manufactured rails, provided that the standard values for the molten mass and finished hardened steel required for the manufacture of the rails are met.

By knowing the composition of the reclaimed rail material, the manufacturer can determine in advance, based on the secondary raw materials available, the composition of the charged material to be remelted and the need for additional interventions (alloying, dilution) to ensure that the rail material produced meets the strict specifications.

It is also possible to check the exact composition of the charged material in the liquid state based on the standard composition to decide on possible further alloying/hardening to achieve the right rail material quality. The concept presented here means a well-planned operation with predictability based on a contract between the manufacturer and the track owner. As a medium-term objective, primary materials can be substantially reduced but not eliminated, bearing in mind that more intensive track development needs may arise, generating additional rail production. There is also a significant material loss due to rail wear and grinding.

Although the results provided by the shown method are validated, they are advanced nonlinear 3D numerical modeling; comparing them with the results in [39] would be helpful. In addition, the rail-wheel relation and other influences on the spindle-rail connection will be considered in further research, which will address specific issues [40].

Although the results provided by the introduced method are validated, comparing them with results from advanced nonlinear 3D numerical modelling, presented in [39] would be helpful. In addition, the authors plan to consider other effects arising

from the rail-wheel relationship in further research, precisely the issues addressed by [40]. In the authors' presented method, the rail head shear stress inside the rail head is considered in detail, while the value at the rail head is only mentioned in order of magnitude. It's probable magnitude is almost the same as the in-rail shear's, so further investigation is needed. The paper [41] has discussed in detail the effect of in-rail stresses on forming RCF faults. Based on their results, the focus of research will be partly shifted to a more precise investigation of this issue, as well as to the issue of natural wear, which they suggest can influence the intensity of the process. The relationship between wear and contact stresses on the surface is reflected in [42]. A complex study of the processes and their consequences, together with the careful application of machining options, can lead to an increase in the service life of the rails, the basis of which is discussed in [43]. A complex overview of the consequences opens up new possibilities for sustainability interpretations [44] [45].

Conclusions

In preparing this article, the authors have explored in detail the calculation of the magnitude of rolling contact fatigue stresses, which are the most common cause of rail failure. Based on the calculation model, they have come to the obvious conclusion that without a significant reduction in the through-capacity of the railway track (not economically feasible), the problem cannot be solved but can only be managed. In this sense, track maintenance is a day-to-day task for track managers. As a result of the combined effects of natural wear and corrective grinding, the rails can only be kept in service for a limited period (first and/or second use cycle), depending on their wear. At the end of it's service life, high-alloy rail steel is sold as simple scrap and recycled as normal steel. Current practice discourages the conscious use of scrap rail. In this article, the authors have proposed the basis for a new type of approach that could lead to a much cheaper and more environmentally friendly production of rails in the spirit of sustainability.

Significant cost and environmental burden reductions can be achieved by considering the following aspects: (i) keeping the rail-wheel contact geometry close to the ideal position, by using Anti-Head-Check profiles and preventive rail machining on the track side; on the vehicle side by continuous maintenance of the wheel profiles; (ii) continued use and proper maintenance of reclaimed track materials in the second use cycle; (iii) reducing production costs by recycling scrap rail steel as rail steel.

Acknowledgment

The authors thank Mag. phil. Z. Mondok for translating the article.

References

[1] Fischer, S., & Kocsis Szürke, S. (2023) Detection process of energy loss in electric railway vehicles. *Facta Universitatis, Series: Mechanical Engineering*, *21*(1), 81-99

[2] Fischer, S., Harangozó, D., Németh, D., Kocsis, B., Sysyn, M., Kurhan, D., & Brautigam, A. (2023) Investigation of heat-affected zones of thermite rail welding. *Facta Universitatis, Series: Mechanical Engineering*. https://doi.org/10.22190/FUME221217008F

[3] Brautigam, A., Szalai, S., & Fischer, S. (2023) Investigation of the application of austenitic filler metals in paved tracks for the repair of the running surface defects of rails considering field tests. *Facta Universitatis, Series: Mechanical Engineering.* https://doi.org/10.22190/FUME230828032B

[4] Németh, A., Fischer, S. (2021) Investigation of the glued insulated rail joints applied to CWR tracks. *Facta Universitatis, Series: Mechanical Engineering*, *19*(4), 681-704

[5] Kuchak, A. T. J., Marinkovic, D., & Zehn, M. (2021) Parametric investigation of a rail damper design based on a lab-scaled model. *Journal of Vibration Engineering Technologies*, *9*, 51-60

[6] Kuchak, A. T. J., Marinkovic, D., & Zehn, M. (2020) Finite element model updating–Case study of a rail damper. *Structural Engineering and Mechanics*, *73*(1), 27-35

[7] Major, Z., Ibrahim, S. K., Rad, M. M., Németh, A., Harrach, D., Herczeg, G., Szalai, S., Kocsis Szürke, S., Harangozó, D., Sysyn, M., Kurhan, D., Baranyai, G., Gáspár, L., & Fischer, S. (2023) Numerical Investigation of Pre-Stressed Reinforced Concrete Railway Sleeper for High-Speed Application. *Infrastructures*, *8*(3), 41

[8] Németh, A., Ibrahim, S. K., Movahedi Rad, M., Szalai, S., Major, Z., Kocsis Szürke, S., Jóvér, V., Sysyn, M., Kurhan, D., Harrach, D., Baranyai, G, Fekete, I., Nagy, R., Csótár, H., Madarász, K., Pollák, A., Molnár, B., Hermán, B., Kuczmann, M., Gáspár, L., & Fischer, S. (2024) Laboratory and Numerical Investigation of Pre-Tensioned Reinforced Concrete Railway Sleepers Combined with Plastic Fiber Reinforcement. *Polymers*, *16*(11), 1498

[9] Ézsiás, L., Tompa, R., & Fischer, S. (2024) Investigation of the Possible Correlations Between Specific Characteristics of Crushed Stone Aggregates. *Spectrum of Mechanical Engineering and Operational Research*, *1*(1), pp. 10-26

[10] Fischer, S. (2023) Evaluation of inner shear resistance of layers from mineral granular materials. *Facta Universitatis, Series: Mechanical Engineering*. https://doi.org/10.22190/FUME230914041F

[11] Eller, B., Szalai, S., Sysyn, M., Harrach, D., Liu, J., & Fischer, S. (2024) Advantages of Using Concrete Canvas Materials in Railway Track Construction. *Naukovyi Visnyk Natsionalnoho Hirnychoho Universytetu*, *2024*(1), 50-57

[12] Eller, B., Szalai, S., Sysyn, M., Harrach, D., Liu, J., & Fischer, S. (2023) Inner Shear Resistance Increasing Effect of Concrete Canvas in Ballasted Railway Tracks. *Naukovyi Visnyk Natsionalnoho Hirnychoho Universytetu*, *2023*(2), 64-70

[13] Sadri, M., & Steenbergen, M. (2018) Effects of railway track design on the expected degradation: Parametric study on energy dissipation. *Journal of Sound and Vibration*, *419*, 281-301

[14] Belalia, A., Kamla, Y., Amara, M., Meliani, M. H., El Azizi, A., & Azari, Z. (2020) Experimental and numerical investigation of UIC 54 rail degradation. *Engineering Failure Analysis*, *111*, 104163

[15] Popović, Z., Lazarević, L., Mićić, M., & Brajović, L. (2022) Critical analysis of RCF Rail Defects Classification. *Transportation Research Procedia*, *63*, 2550-2561

[16] Popović, Z., Mićić, M., & Lazarević, L. (2022) Guidelines for rail reprofiling. *Transportation Research Procedia*, *63*, 2562-2570

[17] Woon, K. S., Phuang, Z. X., Taler, J., Varbanov, P. S., Chong, C. T., Klemeš, J. J., &; Lee, C. T. (2023) Recent advances in urban green energy development towards carbon emissions neutrality. *Energy*, *267*, 126502

[18] Wang, K., Liu, H., Cheng, L., Bian, Z., &; Circella, G. (2022) Assessing the role of shared mobility services in reducing travel-related greenhouse gases (GHGs) emissions: Focusing on America's Young Adults. *Travel Behaviour and Society*, *26*, 301-311

[19] Erdeiné Késmárki-Gally, S., Erdei, A., & Neszmélyi, G. I. (2020) Historical overview of rail passenger transport relations between Hungary and Romania. *Földrajzi Közlemények*, *144*(4), 363-379 (in Hungarian)

[20] Erdei, A., & Erdeiné Késmárki-Gally, Sz. (2018) Development of China's railway connections in the 21st century. In: Neszmélyi Gy. I.: Regional integration and spatial processes in the World. Szent István University Faculty of Economic and Social Sciences, Gödöllő, 27-41

[21] Huang, Y., Ouyang, H., Pan, W., &; He, X. (2023) Role of high-speed rail services in China's economic recovery: Evidence from manufacturing firm inventories. *Economic Analysis and Policy*, *78*, 389-405

[22] Wiedenhofer, D., Baumgart, A., Matej, S., Virág, D., Kalt, G., Lanau, M., Tingley, D. D., Liu, Z., Guo, J., Tanikawa, H., &; Haberl, H. (2023) Mapping and modelling global mobility infrastructure stocks, material flows and their embodied greenhouse gas emissions. *Journal of Cleaner Production*, *434*, 139742

[23] Erdeiné Késmárki-Gally, Sz., Erdei, A., & Grotte, J. (2021) The challenges of Hungarian rail passenger transport in the changing Europe. *Európai Tükör*, *3*, 77-101

[24] McGarry, H., Martin, B., Winslow, P. (2022) Delivering low carbon concrete for network rail on the Routemap to Net Zero. *Case Studies in Construction Materials*, *17*, e01343

[25] Damián, R., & Zamorano, C. I. (2023) Life cycle greenhouse gases emissions from high-speed rail in Spain: The case of the Madrid-Toledo line. *Science of The Total Environment*, *901*, 166543

[26] Vasa, L., Angeloska, A., & Trendov, N. M. (2017) Comparative analysis of circular agriculture development in selected Western Balkan countries based on sustainable performance indicators. *Economic Annals-XXI*, *168*(11-12), 44-47

[27] Vasa, L. (2020) The concept of the circular economy: a trend for the future or a return to basics?, *Valóság: Társadalomtudományi Közlöny*, *63*(3), 1-12 (in Hungarian)

[28] Didenko, I., Valaskova, K., Artyukhov, A., Lyeonov, S., & Vasa, L. (2022) Quality of scientific activity as a determinant of socio-economic development. *Economics and Sociology*, *15*(3), 301-318

[29] Esveld, C. (2001) Modern Railway Track, *MRT-Productions*, Zaltbommel, 654 p.

[30] Kazinczy L. (2000) Investigation of the Hertzian contact stress between the wheel and the rail for railway superstructures, *Műszaki Szemle*, *3*(9-10, 12-16 (in Hungarian)

[31] Ponomarjov, S. D. (1965) Strength calculations in mechanical engineering, Vol. 3, *Műszaki Könyvkiadó*, Budapest, 484 p. (in Hungarian)

[32] Faber G. (1964) Welded Structures, *Műszaki Könyvkiadó*, Budapest, 839 p. (in Hungarian)

[33] Béres L., Unyi B. (1978) Welding of rails, *Műszaki Könyvkiadó*, Budapest, 211 p. (in Hungarian)

[34] Csizmazia F., Horvát F. (2014) Management of rail head damage defects, development of maintenance technology. Definition of technical requirements considering economic aspects, R&D report, 2013-2014 (in Hungarian)

[35] Horváth, R. (2018) Experience of mechanized railway maintenance, *XIX. Conference on Transport Development and Investment*, Bükfürdő, 2018 (in Hungarian)

[36] Mićić M., Brajović L., Lazarević L., Popović Z. (2023) Inspection of RCF rail defects - Review of NDT methods. *Mechanical Systems and Signal Processing*, *182*, 109568

[37] Bollobás J. (2015) Manufacture of standard-gauge railway rails (Part 1) - Technical information content of Hungarian track markings, *Sínek Világa*, *57*(6), 22-26 (in Hungarian)

[38] Taszner Z. (2007) Optimization of the scrap composition technology for converter steelmaking by developing an indirect steel scrap composition method, Miskolc, 2007 (in Hungarian)

[39] Masoudi Nejad, R. (2020) Numerical study on rolling contact fatigue in rail steel under the influence of periodic overload. *Engineering Failure Analysis*, *115*, 104624

[40] Bernal, E., Spiryagin, M., Vollebregt, E., Oldknow, K., Stichel, S., Shrestha, S., Ahmad, S., Wu, Q., Sun, Y., & Cole, C. (2022) Prediction of rail surface damage in locomotive traction operations using laboratory-field measured and calibrated data. *Engineering Failure Analysis*, *135*, 106165

[41] Zhao, X. J., Chen, Q., Liu, Y. S., Qiu, X. Y., Meli, E., & Rindi, A. (2022) Effects of slip ratio and contact stress on rolling contact fatigue of defected rail materials. *Engineering Failure Analysis*, *131*, 105817

[42] Aquib Anis, M., Srivastava, J. P., Duhan, N. R., & Sarkar, P. K. (2018) Rolling contact fatigue and wear in rail steels: An overview. *IOP Conference Series: Materials Science and Engineering*, *377*, 012098

[43] Major, Z., Horváth, R., &; Horvát, F. (2023) Head Checks and the Useful Life of Rails. *Chemical Engineering Transactions*, *107*, 295-300

[44] Harangozó, G. (2008) What makes a company green–or what does good environmental performance mean? *Budapest Management Review*, *39*(1), 27-36

[45] Radácsi, L. (2021) Felelős és fenntartható vállalat. SALDO Kiadó, Budapest, 266 p.